Statistical Analysis of Apparent Fibre Density: Supra-threshold clustering over space and orientation

D. Raffelt[1,2], J-D. Tournier[3,4], G. Ridgway[5], S. Rose[6], R. Henderson[7], S. Crozier[2], A. Connelly[3,4], and O. Salvado[1]

[1]The Australian E-Health Research Centre, CSIRO, Brisbane, QLD, Australia, [2]Biomedical Engineering, School of ITEE, University of Queensland, Brisbane, QLD, Australia, [3]Brain Research Institute, Florey Neuroscience Institutes (Austin), Melbourne, VIC, Australia, [4]Department of Medicine, University of Melbourne, Melbourne, VIC, Australia, [5]Institute of Neurology, University College London, London, United Kingdom, [6]Centre for Advanced Imaging, University of Queensland, Brisbane, QLD, Australia, [7]Department of Neurology, Royal Brisbane and Women's Hospital, Brisbane, QLD, Australia

Introduction: Apparent Fibre Density (AFD) [1] is a novel measure that enables analysis of high angular resolution diffusion-weighted images [2]. Analysis of AFD exploits information provided by Fibre Orientation Distributions (FOD) computed using Spherical Deconvolution [3]. Any differences in the FOD amplitude along a given orientation can be attributed to differences in the relative *amount of underlying axons* thought to be aligned with this orientation [1]. The amount of axons for a given orientation is referred to as '*Apparent*' Fibre Density because it is not an absolute measure of density. Unlike other measures such as Fractional Anisotropy (FA) [4], AFD enables voxel based analysis to be performed over space *and* orientation, and therefore population differences may be attributed to a single fibre population within a voxel containing multiple fibres.

In previous work, differences between populations were detected by comparing the AFD of spatially normalised FODs along corresponding directions [1]. For example, consider the group-wise comparison of FODs located in a single voxel represented by a group 1 mean FOD shown in Fig. 1a, and group 2 mean FOD in Fig. 1b. In [1], AFD was compared by sampling FODs along a number, n, of equally distributed directions (Fig. 1d), followed by a t-test resulting in a t-statistic per direction (Fig. 1c). As shown in Fig. 1c, large t-statistics are observed along directions where differences between the groups exist.

Making n comparisons within each voxel increases the number of multiple comparisons. In [1], significant orientations were computed by performing a Bonferroni correction within each voxel only. In this work, we present a new method for cluster-based inference of spatially extended voxel-wise differences in AFD.

Methods: Cluster-based testing is a popular method for statistical analysis when the spatial extent of group differences is greater than that of noise. One method for assigning statistical significance to regions of extended signal is permutation testing [5]. Here we extend cluster-based permutation testing by thresholding the t-statistics computed along n directions (Fig. 1c), and identifying clusters of contiguous supra-threshold directions by defining neighbours in both space and orientation. Unique clusters of supra-threshold directions were first identified in the spatial domain using ITK 3D connected components filter (6-connected neighbours) [6]. All 3D clusters within each direction were then merged with co-located clusters found in neighbouring directions in the orientation domain (identified as those directions within 20 degrees). We used 100 directions computed with electrostatic repulsion [7] which results in typically 6 neighbours (Fig. 1d).

We created a FOD phantom to investigate the ability of the method to identify a cluster along a fibre bundle with curvature, and to identify two clusters in the same location but at different orientations. Shown in Fig. 1e is a simulated t-statistic image that might be computed from two groups of FOD phantoms with different AFD (generated along 100 directions visualised using spherical harmonics). The t-statistic image was threshold at $t > 2$, and clusters were computed as described above.

The proposed method was applied to a cohort of 13 motor neurone disease (MND) patients and 13 age and gender matched healthy volunteers (3T Siemens Trio, 64 DW directions, b=3000 s/mm^2, 2.3mm in-plane resolution, 2.5mm slice thickness). Pre-processing involved EPI distortion correction [8], bias field correction based on b=0 [9], motion correction (mutual information towards a b=0 with gradient reorientation), mean DW intensity normalisation across subjects, and up-sampling the image resolution by a factor of 2 (cubic b-spline interpolation). FODs were computed using MRtrix [10], and spatially normalised towards an unbiased group average template [11]. During registration we used the Jacobian matrix at each point in the displacement field to reorient the FODs [11]. Because the non-linear registration process alters a fibre bundle's total volume and therefore its total AFD, when applying the final transformations we included an extra step in the reorientation process that modulates the AFD by an amount proportional to the corresponding change in cross-sectional area (and hence in axonal density) [2]. Before computing the AFD along 100 directions, FODs were smoothed in the spatial domain (4mm FWHM Gaussian kernel), and in the orientation domain (truncating FOD spherical harmonic coefficients to degree 4). Analysis was performed using 2000 permutations with a cluster forming threshold of t=1.3. Such a low threshold was selected due to the large spatial extent expected in MND, and relatively small number of subjects; low cluster forming thresholds are unsuitable for random field theory based cluster inference [13], but appropriate for permutation-testing used here.

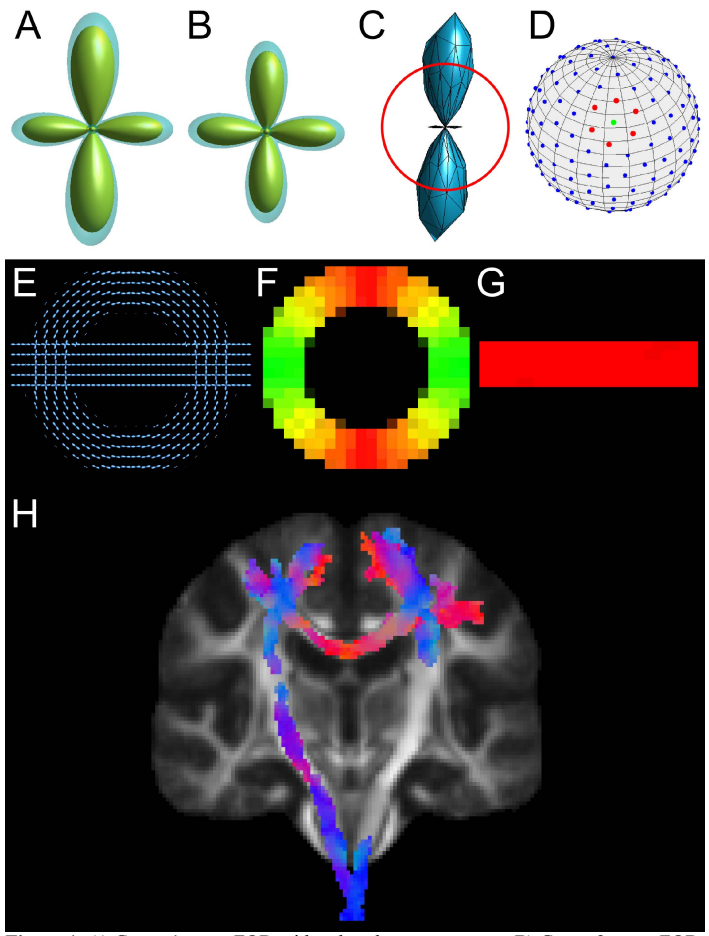

Figure 1. A) Group 1 mean FOD with stdev shown as opaque. **B)** Group 2 mean FOD. **C)** t-statistic computed between FODs in A & B over 100 directions, a hypothetical cluster forming threshold is shown in red. **D)** 100 non-collinear directions. Using a 20 degree cut-off each direction has ~6 neighbours. **E)** Simulated t-statistic image indicating a group difference in a ring fibre bundle, and a bar fibre bundle. **F)** Supra-threshold cluster computed from E, colour coded by cluster mean orientation. **G)** A second supra threshold cluster computed from E. **H)** Two significant clusters ($p<0.03$) identifying a difference in AFD between 13 MND subjects and 13 controls. To visualise the entire cluster, significant directions were averaged along the A-P axis, colour coded for direction, and overlaid on the FA slice shown.

Results: In the simulations (Fig 1e-g), two separate, yet spatially overlapping clusters where correctly identified. To permit direction encoded colouring of the clusters, the mean supra-threshold direction in each voxel was computed and used for display. In the in-vivo MND data, two significant clusters ($p < 0.03$) were detected, (shown in a coronal view on Fig. 1h), identifying voxels and orientations where a decrease in AFD was observed in MND compared to healthy subjects. The clusters are located in the corticospinal tract (CST), and corpus collosal fibres (CC) connecting the primary motor cortices. Both of these regions are known to be affected in MND [12]. Note that the superior cluster contains voxels belonging to both the CC and CST; this is a consequence of both fibre bundles terminating in the superior motor cortex.

Conclusion: We have presented a novel method for cluster-based inference of voxel-wise differences in AFD and demonstrated its ability to detect significant differences between MND and healthy subjects. Being able to detect significant differences in both space and orientation enables more specific conclusions to be drawn, particularly in regions that contain crossing fibres.

References: **[1]** Raffelt D et al. Proc ISMRM #575 (2010). **[2]** Tuch D et al. MRM 48: 577-82 (2002). **[3]** Tournier J et al. Neuroimage 35: 1459-72 (2007). **[4]** Basser P. NMR in Biomed 8: 333-334 (1995). **[5]** Nichols et al. HBM 15:1-25 (2001). **[6]** ITK, www.itk.org. **[7]** Jones D et al. MRM 42: 515-525 (1999). **[8]** Jenkinson, M. MRM 49: 193-7 (2003). **[9]** Salvado O et al. TMI 25: 539-52 (2006). **[10]** MRtrix. www.brain.org.au/software/. **[11]** Raffelt D et al. Proc ISMRM #3969 (2010). **[12]** Agosta F et al. AJNR ajnr.A2043 (2010). **[13]** Hayasaka S et al. Neuroimage 20: 2343-56 (2003).